

Aspects of collisionless magnetic reconnection in asymmetric systems

Michael Hesse¹, Nicolas Aunai¹, Seiji Zenitani², Masha Kuznetsova¹, and Joachim Birn³

¹Heliophysics Science Division, Code 670, NASA Goddard Space Flight Center, Greenbelt, Maryland, 20771, USA

²National Astronomical Observatory of Japan, Tokyo, Japan

³Space Science Institute, Boulder, CO, USA

Asymmetric reconnection is being investigated by means of particle-in-cell simulations. The research has two foci: The direction of the reconnection line in configurations with nonvanishing magnetic fields; and the question why reconnection can be faster if a guide field is added to an otherwise unchanged asymmetric configuration. We find that reconnection prefers a direction, which maximizes the available magnetic energy, and show that this direction coincides with the bisection of the angle between the asymptotic magnetic fields. Regarding the difference in reconnection rates between planar and guide field models, we demonstrate that a guide field can provide essential confinement for particles in the reconnection region, which the weaker magnetic field in one of the inflow directions cannot necessarily provide.

I. INTRODUCTION

Magnetic reconnection, arguably one of the most fundamental energy conversion and transport mechanisms in collisionless plasmas, has traditionally been studied in symmetric systems. We here define symmetric systems to refer to reconnection configurations, in which inflow conditions on both sides are essentially identical, save for sign changes of some magnetic field and velocity components. For these symmetric systems, we have learned a large number of important facts. Specifically, we now know that reconnection is typically fast¹, even though the rate may vary depending on the presence of magnetic islands², and reconnection appears to be mediated by thermal inertia effects, which most prominently manifest themselves in form on nongyrotropic behavior of charged particles of all types, including electrons^{3,4}. We further understand that the reconnection electric field is self-consistently required to maintain both current density and plasma pressure in the diffusion region⁵, and that a substantial component of outflow energy is in form of enthalpy flux^{6,7}.

Strictly speaking, however, symmetric systems are an exception, even though they are often seen as a good approximation to the night side of Earth's magnetosphere. For example, the other important locus of reconnection in the magnetosphere, the magnetopause, is typically far from symmetric due to the interfacing between the radically different plasmas from the magnetosphere and the magnetosheath. Furthermore, the magnetic field of the magnetospheric side typically owes its direction to the Earth's

dipole, whereas the impinging magnetosheath field can have arbitrary directions. The magnetopause, as well as many other systems, is therefore not necessarily well described by what we have learned for symmetric systems. These facts have not gone unnoticed: past research has addressed this problem, beginning with some very early reconnection research⁸⁻¹⁰.

In recent years, magnetic reconnection in asymmetric systems has again begun to attract the attention of researchers interested in the reconnection problem itself. Beginning with MHD-based analyses of balance equations⁶, including the “Cassak-Shay” theory¹¹, reconnection theory and modeling has since been extended into the kinetic realm. Kinetic studies find substantial differences between symmetric and asymmetric reconnection: Pritchett¹² describes an electric field structure very different from symmetric systems; and Mozer and Pritchett¹³ question the relevance of the reconnection electric field in the context of much larger structure of much stronger electric fields.

Despite this initial progress, many open questions remain, however. In this paper, we address two of them. First, we will employ particle-in-cell simulations to determine the X-line orientation, for which the reconnection rate becomes maximum. This will be analyzed for a configuration, which exhibits, in a suitable frame, a constant guide magnetic field. Based on the simulation results and a reasonable physical assumption we will develop a scaling parameter, which varies proportional to the maximum reconnection rate for each simulation frame orientation. We will also show that the coordinate frame with maximum reconnection rate is identical to the one, for which the X-line bisects the two external magnetic field directions.

The second question is related to an observation seen in the reconnection rates of an earlier study¹²: Why does magnetic reconnection exhibit a higher rate in the presence of a guide field than without it, if the system is asymmetric? The common expectation is that the introduction of a significant guide field will reduce plasma compressibility, and hence the available evolution space of the system. Since a more constrained system should evolve more slowly, the observed speedup is a puzzle. We will present an analysis of simulation results to show that, for sufficiently asymmetric systems, the constraining effect a guide field can have on particle orbits can actually be beneficial for the reconnection rate.

The present paper is organized as follows: In section II, we introduce the modeled system, and the numerical model employed for the task. Section III will present results and analyses pertaining to the orientation problem, and section IV will be devoted to the comparative study of guide-field and co-planar simulations. Finally, section V will contain a summary and outlook.

II SYSTEM AND MODEL

We employ dimensionless quantities throughout this paper. The magnetic field is normalized by a typical value B_0 , and densities by a typical density n_0 . Ions are normalized by the proton mass (m_p), and length scales are normalized by the ion inertial length c/ω_i , where the ion plasma frequency $\omega_i = \sqrt{e^2 n_0 / \epsilon_0 m_p}$ is evaluated for the reference density. Velocities are given in terms of the ion Alfvén velocity $v_A = B_0 / \sqrt{\mu_0 m_p n_0}$ based on the reference magnitudes of magnetic field and density.

Consequently, electric field units are $E_0 = v_A B_0$, and the current density is normalized to $j_0 = \omega_i B_0 / c \mu_0$.

The system parameters are set up similar to the choices of Pritchett¹². The poloidal magnetic field is of the following form:

$$B_x = 0.5 + \tanh[z/l] \quad (1)$$

and the initial ion and electron densities are:

$$n_i = n_e = 1 - \tanh[z/l]/3 - \tanh^2[z/l]/3. \quad (2)$$

with $l=0.5$ defining the initial current layer half-width. A constant initial temperature of $T=T_i+T_e=1.5$ is used, with $T_e/T_i=0.2$. A small, X-type, initial perturbation is introduced into current density and magnetic fields, leading to an amplitude $\delta B=0.1$ of the perturbation magnetic field. The initial electric field is set to zero.

Particles are initialized as drifting Maxwellians with temperatures, densities, and drift velocities given by the above parameters. The lack of an exact equilibrium leads to some initial wave activity, which dies down within a few ion cyclotron times.

The system size is chosen to be $L_x=64$ and $L_z=25.6$. In the present study, we employ two choices of constant magnetic field component (“the guide field”) directed along the main current flow

$$B_y = B_{y0} = 0,1 \quad (3)$$

We will refer to the so-defined standard cases of as “co-planar,” and “guide field,” respectively.

In addition to investigating the standard cases, we further study the guide field model in different coordinate systems, derived from the one above by rotation around the z -axis. The rotation angle a is defined in Figure 1. For each simulation in a rotated coordinate system, the entire set of vector quantities defined above is transformed into the rotated coordinate system, and the model is initialized accordingly.

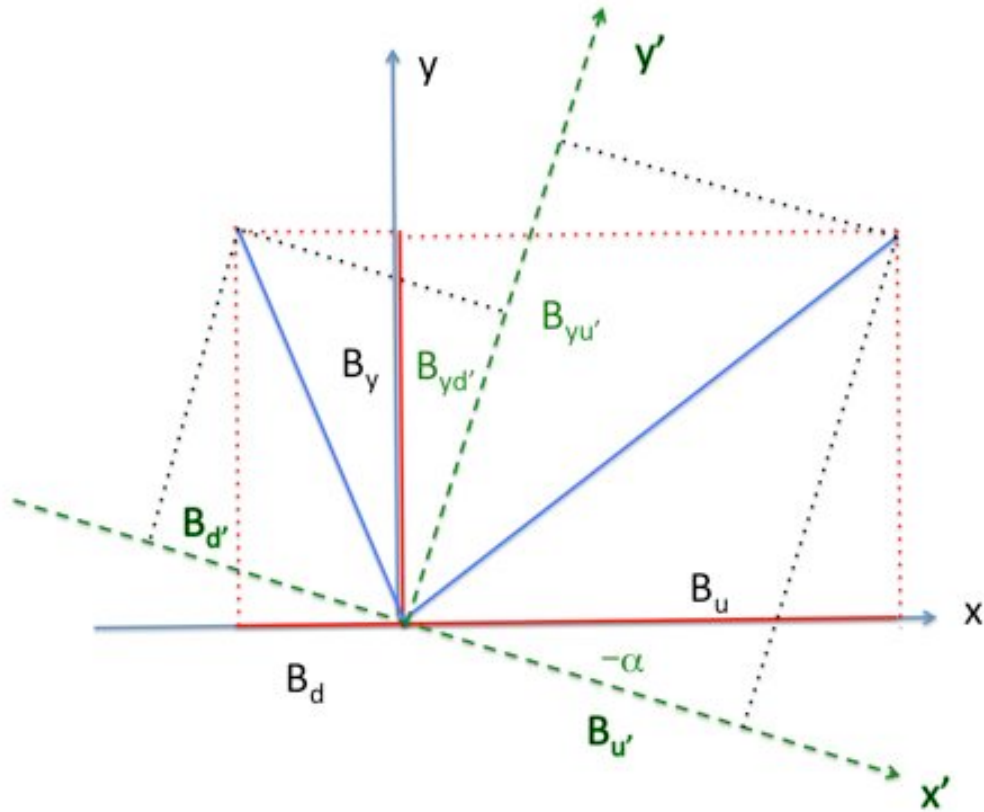


Figure 1. (color online) Representation of the asymptotic magnetic field values in a coordinate system rotated by an angle a about the z axis. The indices ‘ u ’ and ‘ d ’ refer to asymptotic values above and below the current layer, respectively. The globally constant

guide field $B_y=1$ for $\alpha=0$ becomes spatially dependent after rotation. The asymptotic values are shown on the y' axis.

The system evolution is modeled by our particle-in-cell code³. Particle orbits are explicitly calculated in the in the electromagnetic fields, and the electromagnetic fields are integrated by an implicit method on a grid composed of 1000×800 cells in x - and z -directions, respectively. Periodic boundary conditions are employed in the x direction, whereas the particles are specularly reflected at the upper and lower boundaries. The ion-electron mass ratio is chosen to be $m_i / m_e = 25$. The ratio between plasma and electron gyrofrequency is set to $\omega_{pe} / \omega_{ce} = 4$ and the time step is $dt = 0.2$. A total of 1.6×10^9 macro-particles are employed during each calculation.

III RECONNECTION RATE AND X-LINE ORIENTATION

We investigate the reconnection behavior by means of a set of simulations performed for different values of the coordinate system rotation α . The overall evolution of the reference system, with uniform guide field of unity (i.e., $\alpha=0$), is illustrated for three different times in Figure 2. The figure shows a transition from initially symmetric behavior to the development of a significant left-right asymmetry toward the end of the simulation period ($t=80$).

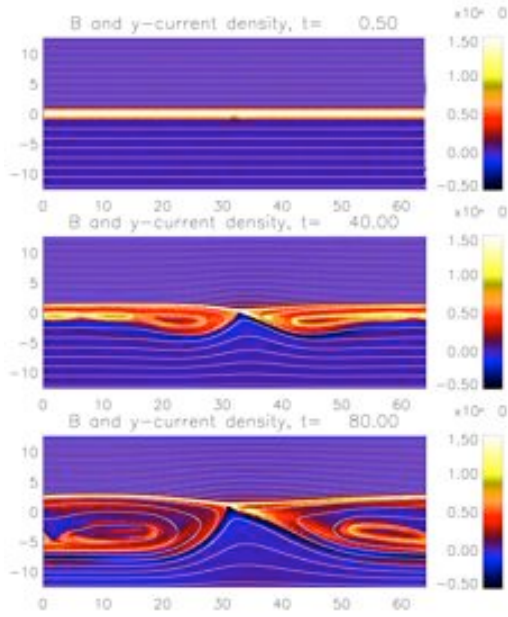


Figure 2. (color online) Magnetic field and current density evolution for the reference run, for which the initial guide field is uniform and of unit value.

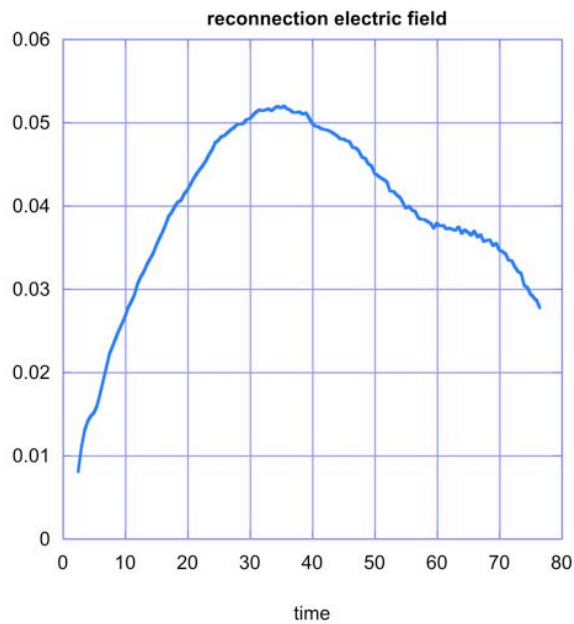


Figure 3. (color online) Time evolution of the reconnection electric field for the reference run, for which the initial guide field is uniform and of unit value.

The temporal evolution of the reference reconnection rate is shown in Figure 3. The figure demonstrates that Sonnerup's⁸ prediction of fast reconnection in the presence of a guide field is correct: the peak reconnection rate is still about 0.05. The key question is whether faster reconnection can be obtained for different X-line orientations. The answer to this question is shown in Figure 4, which displays the time evolution of the reconnection rates for all runs obtained from the guide field reference model by coordinate system rotation.

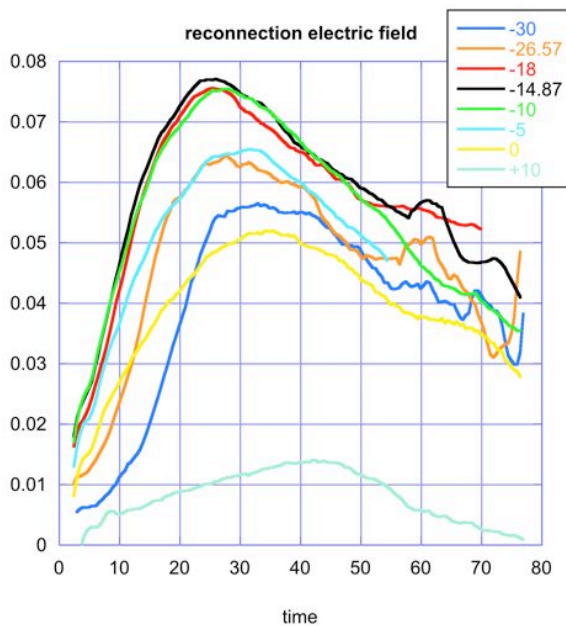


Figure 4. (color online) Time evolution of the reconnection electric field for the entire set of runs derived from rotating the frame of the guide field calculation by an angle α . The different colors denote different runs, and the angles are denoted in the figure.

Fig. 4 displays a strong variation of reconnection rates with choice of coordinate system, with a maximum for $\alpha=-14.87$ degrees. The extremum appears to be weakly localized only: adjacent values of the rotation angle yield almost identical reconnection rates. More negative rotation values lead to rapidly decreasing values of the reconnection electric fields, as do less negative and positive values. It is noteworthy that the reconnection evolution for $\alpha=-26.57$ degrees, for which the reconnection magnetic fields are equal on both sides, still leads considerably slower reconnection rates than the runs for smaller rotation angles. Therefore, symmetry of the in-plane magnetic field does not lead to the fastest reconnection rates.

angle/degrees	empirical peak E
10.000	0.014000
0.0000	0.052000
-5.0000	0.065000
-10.000	0.075400
-14.870	0.077000
-18.000	0.075000
-26.570	0.064000
-30.000	0.057000
-56.364	0.0000

Table 1: Maximum reconnection electric field values for the set of rotation angles considered. The zero value for $\alpha=-56.364$ degrees is not empirical. For this rotation, the upper magnetic field vanishes.

In order to develop a scaling relation for the reconnection electric field, we consider the maximum value of the entire time evolution for a fixed rotation angle. The result is shown in Table 1. We again find a maximum, at least among the runs considered, for $\alpha=-14.87$ degrees. The reconnection rate has to vanish for rotations, for which one of the two rotated magnetic field components:

$$B_{u'} = B_u \cos(\alpha) + B_y \sin(\alpha) \quad (4)$$

$$B_{d'} = B_d \cos(\alpha) + B_y \sin(\alpha) \quad (5)$$

vanishes. For the system investigated here, $B_{u'}=0$ for the rotation value shown at the bottom of table 1.

The key question is how the maximum values shown here relate to physical parameters. We will approach this issue from two different angles. First, we will make a reasonable assumption: reconnection rates should scale with the available magnetic energy. Because of the constancy of the total volume, this assumption implies that reconnection rates should be proportional to the magnetic energy density. Since the energy densities available for reconnection can differ across the current layer, our assumed proportionality implies:

$$E_r = \beta_l B_u^2 B_{d'}^2 \quad (6)$$

where the factor β_l should depend on parameters like density, total magnetic field etc., which are held constant in the present investigation. Using the rotated magnetic field expressions (4) and (5), it is a straightforward exercise to derive the following equation

$$\cot^2 \alpha_{\max} - 2 \frac{B_d B_u - B_y^2}{B_y (B_u + B_d)} \cot \alpha_{\max} - 1 = 0 \quad (7)$$

for the angle α_{\max} , for which (6) attains its maximum. The relevant solution is:

$$\alpha_{\max} = -14.87^\circ \quad (8)$$

It is further interesting to note, that eqn. (7) also describes the angle, which bisects the angle between the asymptotic magnetic field on both sides of the current layer. This result is quite generic: the half-angle direction maximizes the magnetic energy available for reconnection.

As a second approach, we consider the Cassak-Shay formula

$$E_r = \beta_2 \bar{v}_A \bar{B} \quad (8)$$

with the following definitions, in our notation:

$$\bar{v}_A = \sqrt{\frac{B_u B_d}{\bar{\rho}}} \quad (9a)$$

$$\bar{\rho} = \frac{B_u \rho_d + B_d \rho_u}{B_u + B_d} \quad (9b)$$

$$\bar{B} = \frac{2B_u B_d}{B_u + B_d} \quad (9c)$$

The proportionality constants β_1 and β_2 are chosen so that the maximum values of E_r coincide with the maximum value of table 1. The results are shown in Figure 5. The figure shows an excellent match for the magnetic energy-based fit, with significant deviations only for larger angular difference from the ideal rotation value. Surprising at first is the performance of the Cassak-Shay formula. There are at least two possible reasons for this deviation: First, the Cassak-Shay expression was derived for steady state reconnection processes, whereas we are here studying the maximum of a time dependent reconnection process. Second, and perhaps more importantly, kinetic processes may play a significant role in providing reconnection behavior different from fluid models. We are presently not able to prove this argument; however, the results of the following section are supporting this point of view. In summary, our results indicate that the magnetic reconnection line in asymmetric systems is preferentially oriented in such a way that it bisects the direction of the asymptotic magnetic field direction on both inflow sides. This orientation is identical to the one for which the product of available magnetic energy is maximized.

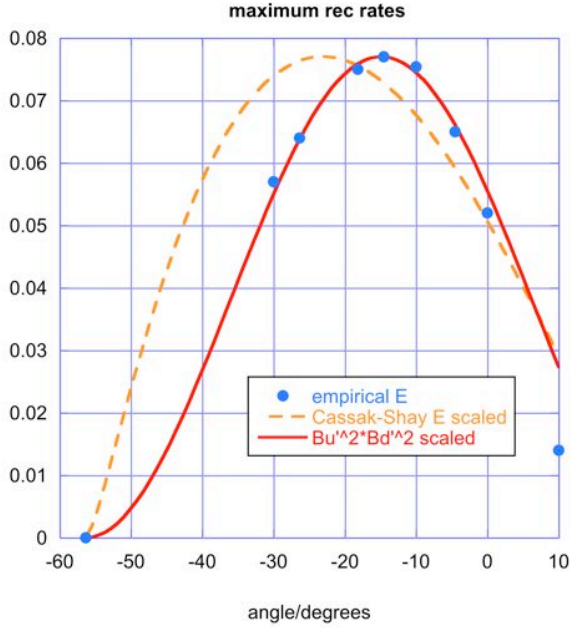


Figure 5. (color online) Plot of peak electric field values from table 1, and predictions based on the Cassak-Shay model, and on the magnetic energy available for magnetic reconnection. The magnetic energy-based prediction exhibits an excellent match.

IV. COPLANAR AND GUIDE-FIELD RECONNECTION

An inspection of Pritchett's paper¹² reveals a puzzling result: in the asymmetric system investigated by him, the addition of a guide magnetic field appears to speed up the magnetic reconnection process, or, conversely, the coplanar model exhibits and anomalously low reconnection rate. We researched this problem using the system described by (1)-(3) and found surprising results: For MHD and Hall-MHD models (not shown) reconnection rates were either not changed or slightly lower in the presence of a guide field, whereas kinetic models results, even for equal mass ratio or in hybrid

simulations (Aunai et al., submitted to Phys. Plasmas) all exhibit slower reconnection rates in the absence of a guide field. Figure 6 shows the time evolution of the reconnection electric fields for the systems described by eqns. (1)-(3) modeled by our particle-in-cell code.

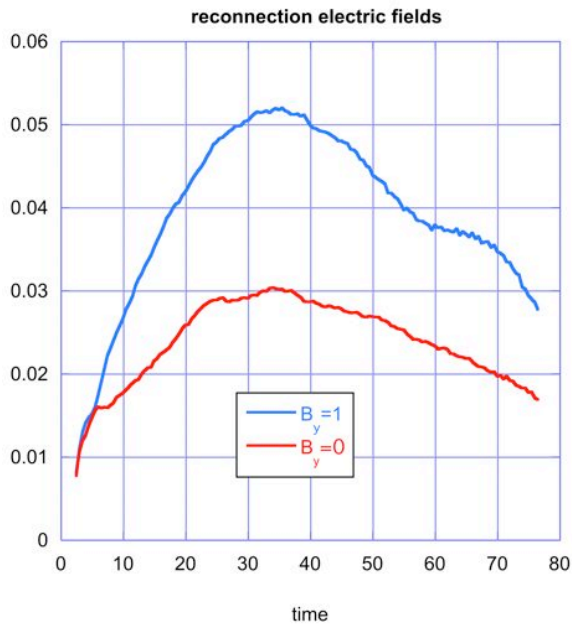


Figure 6. (color online) Reconnection rates for the runs with and without guide field. The only difference between initial conditions is the addition of a guide field of unit value. The reconnection rates for the run without a guide field are about 60% larger.

The substantial difference in reconnection rates, showing an anomalous slowdown in the coplanar model, begs further investigation. The difference between fluid and kinetic models strongly suggests kinetic reasons for the variation in reconnection rates seen here. We will therefore analyze the two simulations for comparable states of their evolution.

Specifically, we pick times for which the amount of magnetic flux, which has been reconnected, is equal. One such selection is $t=80$ for the coplanar calculation, and $t=48$ for the system with a guide field. For comparison, the two states are shown in Figure 7.

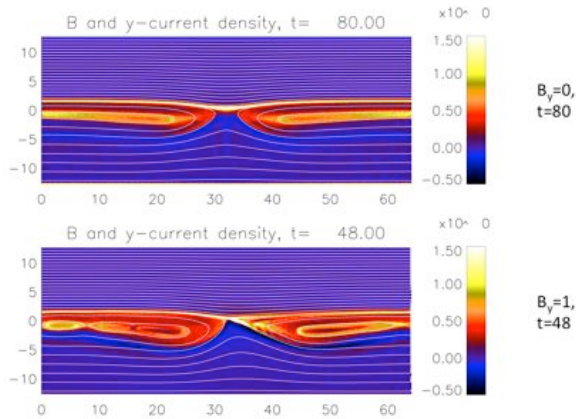


Figure 7. (color online) Times selected for comparison between coplanar (top) and guide field calculation (bottom). The times are selected based on equal amounts of reconnection magnetic flux, i.e., of magnetic flux crossing the initial tangential discontinuity.

Magnetic reconnection involves the conversion of magnetic energy into particle energy in form of heating and bulk kinetic energy. In the diffusion region, the reconnection electric field fulfills two primary functions⁵: it provides current continuity, and it provides sufficient heating to sustain plasma pressure in the high- β current layer. It seems apparent that any such process facilitating magnetic reconnection will operate better if it is highly localized. We will return to this argument below; here we show that the role of the guide field is to provide substantially enhanced localization.

For this purpose, we study the local bounce widths of both ions and electrons. Bounce widths are defined as follows: The upper and lower bounce widths are the locations, where the local particle Larmor radius is equal to the distance (in z) from the position of the magnetic field (B_x) reversal layer for the same x value. More formally, if $z_n(x)$ is the line, for which $B_x(x, z(x))=0$, then the upper and lower bounce widths are the solutions of:

$$\lambda_u(x): \frac{mv_{th}(x, z_n(x) + \lambda_u(x))}{eB(x, z_n(x) + \lambda_u(x))} = z_n(x) + \lambda_u(x) \quad (10a)$$

$$\lambda_d(x): \frac{mv_{th}(x, z_n(x) - \lambda_d(x))}{eB(x, z_n(x) - \lambda_d(x))} = z_n(x) - \lambda_d(x) \quad (10b)$$

Both equations can be evaluated for ions or electrons, i.e., the thermal velocities v_{th} and masses m may represent values for either ions or electrons. Solutions are found by a simple search algorithm, excluding, for the coplanar case, the immediate region where the magnetic field vanishes. The area spanned by the bounce widths as a function of x is identical to the domain, where particles of a given species are unmagnetized.

We will investigate the structure of the unmagnetized regions for both ions and electrons, beginning with the reference times. Figure 8 shows the extent of ion unmagnetization for the two reference times, and Figure 9 shows the same for electrons.

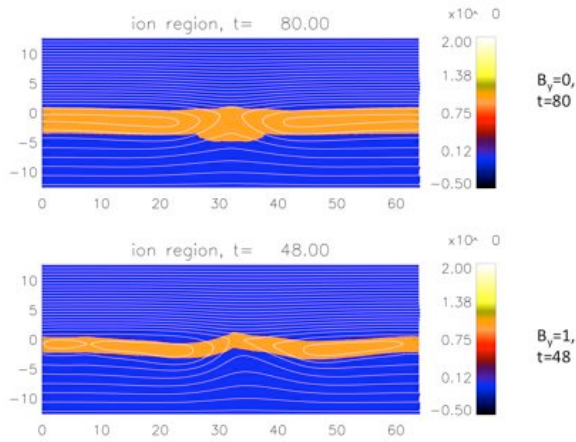


Figure 8. (color online) Ion demagnetization regions for the two reference times. The figure shows a dramatically larger region in the absence of an initial guide field.

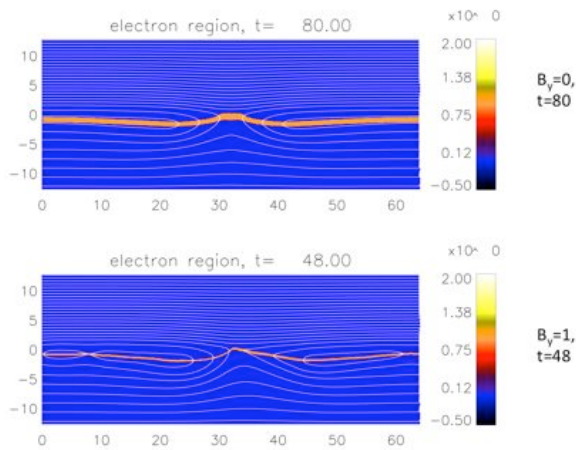


Figure 9. (color online) Electron demagnetization regions for the two reference times. The figure shows a dramatically larger region in the absence of an initial guide field also for electrons.

Both figures exhibit the same qualitative pattern: ions and electrons are much less well confined in the coplanar calculation. This appears to be particularly so in the neighborhood of the X-point, where bounce excursions in the z direction are even larger

than elsewhere. While figs. 8 and 9 show a snapshot in time, figure 10 proves that the same features apply throughout the entire model run.

We therefore find that the magnetic confinement is substantially different in both calculations. The effect of the guide field is to constrain particle motion to a much tighter region around the in-plane (poloidal) magnetic field reversal than the relatively weak B_x below the current layer can accomplish. This effect is even more pronounced at the X-point, where the in-plane magnetic field strength is further reduced by the magnetic reconnection process. In the coplanar model, the ion excursion area becomes multiple ion inertial lengths. We note that, in the symmetric case, the (equal) magnetic field on both sides provides sufficient confinement. Here adding a guide field has no beneficial effect: it will instead slow down reconnection if it is large enough¹⁶, rendering the plasma less compressible.

Here, however, low particle confinement is not conducive for large magnetic reconnection rates. In addition to large gradient scale lengths, large regions of unmagnetization serve to smear out any relevant structures, such as pressure nongyrotropies³, and current densities, over larger areas with reduced amplitudes. Broad regions such as in the coplanar model will prevent the formation of the highly localized diffusion regions, which are required for fast reconnection.

The difference of reconnection electric fields can also be understood when considering the basic physics in the diffusion region. The reconnection electric field has two functions⁵: sustain the current sheet, and sustain the current sheet pressure. Particles will typically spend more time in extended diffusion regions than in highly localized

ones, leaving more time for the reconnection electric field to act on them in the former case. Therefore, there will be, on average, more time to accelerate and heat plasma in transit throughout the diffusion region. However, the total current and plasma sheet pressures are identical or similar, respectively, in the coplanar and guide field calculations at similar evolution levels. The longer acceleration opportunity in the coplanar model therefore requires a weaker reconnection electric field, which is exactly what we find here.

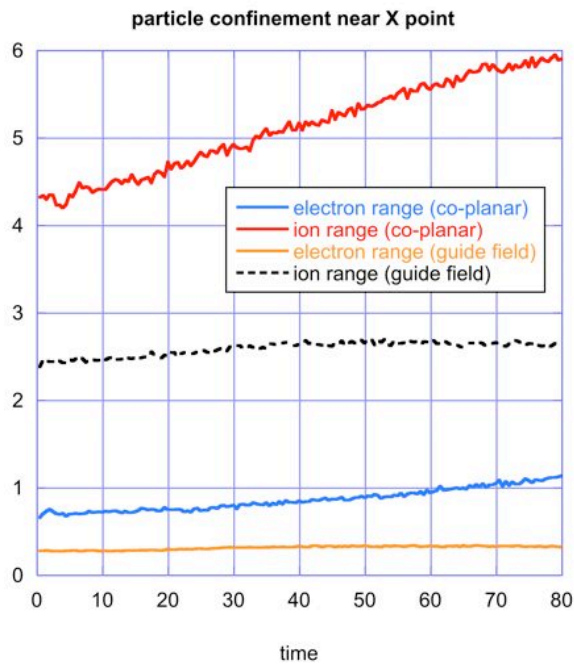


Figure 10. (color online) Time evolution of electron and ion demagnetization region dimensions at the dominant X-point, for the two reference runs. The figure demonstrates that both ions and electrons are substantially less well confined throughout the entire coplanar simulation.

V. SUMMARY AND CONCLUSIONS

The present paper presents a look at two questions regarding magnetic reconnection in asymmetrical systems: the preferred direction of the reconnection line, and the question why reconnection in asymmetrical systems can, at times, be faster with a guide field than without it. We researched these questions in two steps, the first focusing on the direction of the reconnection line, and the second addressing the second topic.

Regarding the direction of the reconnection line, we found a surprisingly good match between simulated reconnection rates and the maximum of the product of the magnetic energy densities in the two inflow regions. Surprisingly, the well-known Cassak-Shay formula¹⁰ did not perform as well; suggested explanations include the time-dependent nature of our calculations, and the possibility of inherent differences between fluid and kinetic models. Resolution of this question will be the subject of future research.

We also showed, by means of simple algebra, that maximizing available magnetic energy is equivalent to halving the angle between asymptotic magnetic fields. Therefore, our results are in support of earlier suggestions^{14,15}, and they provide predictions for spacecraft observations. However, we must caution that the present result, while compelling, has been deduced from a limited set of calculations for a limited range of parameters. In order to increase confidence, additional tests are required, which extend geometry and parameter space systematically, and also extend models to fully three-dimensional calculations. This topic will be the focal area of our subsequent research.

In the second part of the present study, we analyzed the reconnection rates of two asymmetric simulations, which differed only by the presence or absence of a guide (or, out-of-plane) magnetic field component. Contrary to experiences in symmetric systems¹⁶, previous¹² as well as present simulations show faster reconnection with guide field than without it, indicating that the usual, compressibility-based, slow-down may be overcome by other effects.

Through detailed analysis of particle dynamics we identified as the relevant kinetic mechanism the confinement of particles to the field reversal region near the X-point, by the combination of in-plane and guide fields. We argued that substantially larger demagnetization regions should smear out critical reconnection features, such as pressure nongyrotropies. Furthermore, larger diffusion regions should generally require lower reconnection electric fields based on a general argument about current and internal energy continuity⁵. While not proofs in the strictest sense of the word, these ideas are highly plausible as explanation of the discovered morphology.

Further research is required here as well. For example, it seems self-evident that increasing guide fields further and further will eventually overcome the beneficial effects of localization through the detrimental effects of reduced compressibility. It is presently unclear when the rate turnover will occur. As a rough guideline one would expect reductions of the reconnection rate as soon as the guide field provides more magnetic pressure than the stronger of the in-plane magnetic fields, i.e., for

$$B_y > \max(B_u, B_d) \quad (11)$$

but the exact behavior will have to be determined by future research.

The present paper provides evidence in support of two conclusions: First, the direction of the X -line in asymmetric reconnection is such that it bisects the angle between the asymptotic directions of the total magnetic field; and, second, that in some situations, guide field reconnection may be faster than anti-parallel reconnection. Our results are strongly supportive of these conclusions. While a strict, mathematical proof is beyond the scope of the present research, we hope to have provided incentives for further investigations of these two topics. In any case, it appears that kinetic physics plays a rather large role in asymmetric magnetic reconnection.

Acknowledgements: The authors gratefully acknowledge support by NASA's MMS mission and SR&T program. One of us (NA) gratefully acknowledges support from NASA's NPP program.

REFERENCES

- ¹J. Birn, J. F. Drake, M. A. Shay, B. N. Rogers, R. E. Denton, M. Hesse, M. Kuznetsova, Z. W. Ma, A. Bhattacharjee, A. Otto, and P. L. Pritchett, *J. Geophys. Res.*, **106**, 3715 (2001).

- ²H. Karimabadi, W. Daughton, and J. D. Scudder, *Geophys. Res. Lett.*, (2007), L13104, doi:10.1029/2007GL030306 (2007).
- ³M. Hesse, M., K. Schindler, J. Birn, and M. Kuznetsova, *Phys. Plasmas*, **6**, 1781 (1999).
- ⁴M. Hesse, T. Neukirch, K. Schindler, M. Kuznetsova, S. Zenitani, *Space Sci. Rev.*, **160**, pp. 3-23 (2011).
- ⁵M. Hesse, S. Zenitani, M. Kuznetsova, and A. Klimas, *Phys. Plasmas* **16**, 102106 (2009).
- ⁶J. Birn, J. Borovsky, M. Hesse, and K. Schindler, *Phys. Plasmas*, **17**, 052108 (2010).
- ⁷N. Aunai, N., Belmont, G., & Smets, R, *Phys. Plasmas*, **18**, 2901, doi:10.1063/1.3664320 (2011).
- ⁸B. U. O. Sonnerup, *J. Geophys. Res.*, **79**, 1546 (1974).
- ⁹W. D. Gonzales, and F. S. Mozer, *J. Geophys. Res.*, **79**, 4186 (1974)
- ¹⁰S. W. Cowley, *J. Geophys. Res.*, **81**, 3455 (1976).
- ¹¹P. A. Cassak and M. A. Shay, *Phys. Plasmas* **14**, 102114 (2007).
- ¹²P. L. Pritchett, *J. Geophys. Res.* **113**, A06210, DOI: 10.1029/2007JA012930 (2008).
- ¹³F. S. Mozer and P. L. Pritchett, *Space Sci. Rev.*, **158**, 119 (2011).
- ¹⁴D. G. Sibeck, *Ann. Geophys.*, **27**, 895 (2009).
- ¹⁵R. Schreier, M. Swisdak, J. F. Drake, and P. A. Cassak, *Phys. Plasmas* **17**, 110704 doi: 10.1063/1.3494218 (2010).
- ¹⁶J. D. Huba, *Phys. Plasmas*, **12**, 012322 (2005).

FIGURE CAPTIONS

Figure 1 (color online). Representation of the asymptotic magnetic field values in a coordinate system rotated by an angle α about the z axis. The indices 'u' and 'd' refer to asymptotic values above and below the current layer, respectively. The globally constant guide field $B_y=1$ for $\alpha=0$ becomes spatially dependent after rotation. The asymptotic values are shown on the y' axis.

Figure 2. (color online) Magnetic field and current density evolution for the reference run, for which the initial guide field is uniform and of unit value.

Figure 3. (color online) Time evolution of the reconnection electric field for the reference run, for which the initial guide field is uniform and of unit value.

Figure 4. (color online) Time evolution of the reconnection electric field for the entire set of runs derived from rotating the frame of the guide field calculation by an angle α . The different colors denote different runs, and the angles are denoted in the figure.

Figure 5. (color online) Plot of peak electric field values from table 1, and predictions based on the Cassak-Shay model, and on the magnetic energy available for magnetic reconnection. The magnetic energy-based prediction exhibits an excellent match.

Figure 6. (color online) Reconnection rates for the runs with and without guide field. The only difference between initial conditions is the addition of a guide field of unit value. The reconnection rates for the run without a guide field are about 60% larger.

Figure 7. (color online) Times selected for comparison between coplanar (top) and guide field calculation (bottom). The times are selected based on equal amounts of reconnection magnetic flux, i.e., of magnetic flux crossing the initial tangential discontinuity.

Figure 8. (color online) Ion demagnetization regions for the two reference times. The figure shows a dramatically larger region in the absence of an initial guide field.

Figure 9. (color online) Electron demagnetization regions for the two reference times. The figure shows a dramatically larger region in the absence of an initial guide field also for electrons.

Figure 10. (color online) Time evolution of electron and ion demagnetization region dimensions at the dominant X-point, for the two reference runs. The figure demonstrates that both ions and electrons are substantially less well confined throughout the entire coplanar simulation.